Pitched π-stacking crystal structure and two-dimensional electronic structure of acenaphtho[1,2-k]fluoranthene analogues with various substituents

Takuma Yuki,[1] *Seiya Yokokura,*[1,2,*] *Mingoo Jin,*[3] *Hiroki Waizumi,*[1,2] *Taro Nagahama,* [1,2,] *Toshihiro Shimada*[1,2,*]

[1]Graduate School of Chemical Sciences and Engineering, Hokkaido University, Kita 13 Nishi 8, Kita-ku, Sapporo, 060-8628, Japan

[2]Division of Applied Chemistry, Faculty of Engineering, Hokkaido University, Kita 13 Nishi 8, Kita-ku, Sapporo, 060-8628, Japan

[3]Institute for Chemical Reaction Design and Discovery (WPI-ICReDD), Hokkaido University, Sapporo, Hokkaido 060-8628, Japan

Seiya Yokokura[*]**:** seiyayokokura@eng.hokudai.ac.jp

Toshihiro Shimada[*]**:** shimadat@eng.hokudai.ac.jp

SYNOPSIS

7,14-diphenylacenaphtho[1,2-k]fluoranthene (DPAF) and its analogues were synthesized and crystallized. The correlation between substituents and crystal structures and electronic states of the previously reported and synthesized molecules were explored experimentally and theoretically. DPAF crystal was found to form a two-dimensional electronic structure in spite of its pitched π-stacking structure.

ABSTRACT

Electronic properties of organic semiconductors are governed by their crystal structures. Rubrene, a high-mobility organic semiconductor, forms a pitched π-stacking structure. We here focused on 7,14-diphenylacenaphtho[1,2-k]fluoranthene (DPAF), which gives a crystal isomorphic to rubrene. In addition to DPAF, we newly synthesized 7,14-dithienyl-AF (DTAF) and obtained three types of pitched π-stacking structures: the previously reported orthorhombic DPAF (DPAF-O), a new polymorphic monoclinic DPAF (DPAF-M), and DTAF. To investigate factors causing these molecules to form pitched π-stacking structures, the intermolecular interactions of the face-to-face molecular pairs were calculated for these molecules, non-substituted AF and butyl-substituted AF molecules. Unsubstituted AF and butyl-substituted AF have the most stable π-stacking structure with a small misalignment, whereas DPAF and DTAF have the most stable π-stacking structure with a large misalignment along the molecular long axis. Such misaligned π-stack structures are essential for pitched π-stacking structures. Theoretical calculations of the mobility anisotropy based on the hopping model suggested that DPAF-M and DTAF form one-dimensional electronic states, while DPAF-O forms two-dimensional electronic states. Actually, isotropic mobility was observed in SC-FETs with DPAF-O. Collectively, our results indicated that molecular design

which introduces broad π-conjugated moieties at the ends of molecules is effective for enhancing the two-dimensionality of electronic states of pitched π-stacking structures.

Introduction

The electronic properties of organic devices such as organic transistors are governed by the electronic states of the constituent molecules and their packing structures.[1–5] While the π-conjugated skeleton is of course important for high performance organic transistors, the choice of substituents is also very important, even if it does not contribute to charge transport, because the choice of substituents can easily change the molecular packing.[6–8] Even when the same π skeleton is used, the charge mobility can be dramatically changed by modifying the substituents. For example, unsubstituted tetracene forms a herringbone structure [9,10] with a hole mobility of 0.1–2.4 $cm^2 V^{-1} s^{-1}$.[11–15] In contrast, the crystal structure of rubrene modified with four phenyl groups on the tetracene skeleton changes to a pitched π stacking structure with a large transfer integral in the π-stacking direction that results in high mobility.[16–18] Indeed, the mobility of this structure is more than 10 times higher than that of tetracene.[19–22] To obtain high-mobility organic transistors, the design of organic semiconductors with rubrene-like pitched π-stacking structures has long been investigated, but rarely successfully. Recently, Takimiya et al. demonstrated that the packing of molecules into rubrene-like pitched π-stacking can be controlled by β-methylthionization of a series of acendithiophenes.[23–27] Moreover, they showed that these crystals with pitched π-stacking structures have high mobility. Nevertheless, there are very few organic semiconductors that exhibit a pitched π-stacking structure.

The crystal structure of acenaphtho[1,2-k]fluoranthene (AF) varies depending on substituent modifications. Unsubstituted AF molecules and 7,14-diR-AF (R = n-C_3H_7, n-C_4H_9, n-C_5H_{11}) molecules,[28–30] modified with alkyl groups, form 1D π-stacking structures. On the other hand, 7,14-diphenyl-AF (DPAF) molecules modified with phenyl groups (Scheme 1) form pitched π-stacking structures. Therefore, these molecules are useful systems for exploring the correlation

between the formation of pitched π-stacking structures and the type of substituents. Although the mobility of thin-film transistors using 7,14-dicarbethoxy-AF, which forms a 1D π-stacking structure, is not very high ($1.7\times10^{-3}cm^2V^{-1}$),[31] DPAF is expected to show high mobility because it is isomorphous crystal (space group: *Cmca*) with rubrene. While the crystal structure of DPAF has been reported,[32] its electronic properties have not yet been explored. In addition to being the isomorphic crystal of rubrene, compared to the tetracene skeleton of rubrene, the AF skeleton has a wide π-conjugation due to the naphthalene moiety at the end of the molecule, which allows for a large electronic coupling in the end-to-face direction when forming a pitched π-stacking structure. In this study, we demonstrated both experimentally and theoretically that the DPAF crystal has a two-dimensional electronic structure despite its pitched π-stacking structure. In addition to the DPAF, we synthesized a new molecule, 7,14-dithienyl-AF (DTAF), and found that it also has a pitched π-stacking structure. Finally, by comparing the crystal structures and intermolecular interactions of these two types of molecules with previously reported unsubstituted and alkyl-chain introduced molecules, we investigated the factors determining the pitched π-stacking structure.

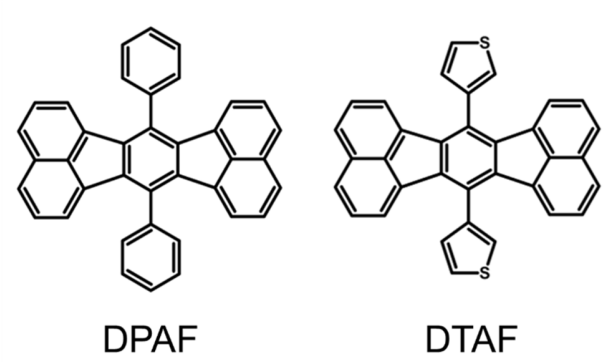

Scheme 1. Molecular structure of DPAF and DTAF

Experimental

Materials

DPAF was synthesized according to the reported procedure, and DTAF was synthesized using the similar procedure as used for DPAF.[33] Both molecules were crystallized by the physical vapor transport (PVT) and naphthalene flux methods.[34–36] Details of the syntheses and the naphthalene flux method are given in the Supporting Information.

Single-crystal X-ray analysis

Single-crystal X-ray structural analyses were carried out with a Rigaku XtaLAB PRO MM007 diffractometer using graphite-monochromated Cu-Kα radiation at 153 K. The structure was solved by direct methods and expanded using Fourier techniques. The non-hydrogen atoms were anisotropically refined. The hydrogen atoms were refined by using the riding model. All calculations were performed using the Olex2[37] crystallographic software package, except for refinement, which was performed using SHELXL-2019/2.[38] The crystal structures and packing motifs were analyzed for visualization by an electronic and structural analysis program.

Theoretical calculation

The molecular orbital calculations were performed using the Gaussian 16W. For the calculation of the electron coupling term (V), the molecular structure extracted from the crystal structure data was used without relaxation, and the calculation conditions were set to B3LYP/6-31G(d,p). For the calculation of the intermolecular interactions, calculated levels of B3LYP/6-31G(d,p) was used, and the basis set superposition error (BSSE) was corrected using the counterpoise method. In addition, empiricaldispersion = gd3 was used to correct for dispersion forces. [39,40] For the reorganization energy (λ) calculation, B3LYP/6-31G(d,p)//B3LYP/6-31G(d,p) was used. With V

and λ, the theoretical mobilities based on the hopping model were calculated in accordance with the literature[41,42].

Single-crystal field effect transistors

Bottom-gate bottom-contact FETs were fabricated using single crystals of DPAF. Heavily doped n-type Si wafers with SiO_2 layers (500 nm) were used as substrates. The substrates were cleaned by sonication in EtOH for 30 min followed by ultraviolet–ozone treatment for 15 min. Then, the substrates were treated with trimethoxy(1H,1H,2H,2H-heptadecafluorodecyl)silane (TCI Chemicals). The Au source and drain electrodes (50 nm) were deposited directly on the substrates by physical vapor deposition under $< 5 \times 10^{-3}$ Pa. The modification of Au electrodes with pentafluorobenzenethiol[43] (PFBT; TCI Chemicals) was performed by immersion in 50×10^{-3} M solution in ethanol overnight under ambient conditions. The DPAF crystals grown by the physical vapor transport method were carefully transferred from the glass tube to the top of the SAM-treated substrates. The field-effect mobility μ was extracted from the saturation regime.

Results and discussion

Crystal structure

Figure 1 shows photographs of the DPAF and DTAF crystals. For DPAF, crystals were obtained by two methods: block crystals (Figure 1a) by the naphthalene flux method and film (Figure 1b) and plate crystals (Figure 1c) by the PVT method. Among these three types of DPAF crystals, block and film crystals have the same pitched π-stacking structure as the crystal structure previously reported (space group: *Cmca*; Figure 2a).[33] The plate-like crystal was found to be a polymorphic crystal (space group: $P2_1/n$; Figure 2b), which has not been reported before. The

former was referred to as the DPAF-O and the latter as the DPAF-M. The lattice parameters are summarized in Table S1. In the DPAF-O, all molecules in the pitched π-stacking layer, which is formed on the *bc* plane as well as the rubrene, are located in a common crystallographic mirror plane (Figure 3a, d). Since the interplanar distance along the π-stacking direction of this crystal (3.478 Å) is smaller than that of rubrene (3.642 Å),[44] greater electronic coupling along this direction can be expected (Figure S4). In addition, the dihedral angle with molecules in the end-to-face direction in DPAF-O (53°) is more acute than that in rubrene (61°), so that the molecular planes are closer to each other, which is expected to increase the electronic coupling in this direction as well (Figure S5).

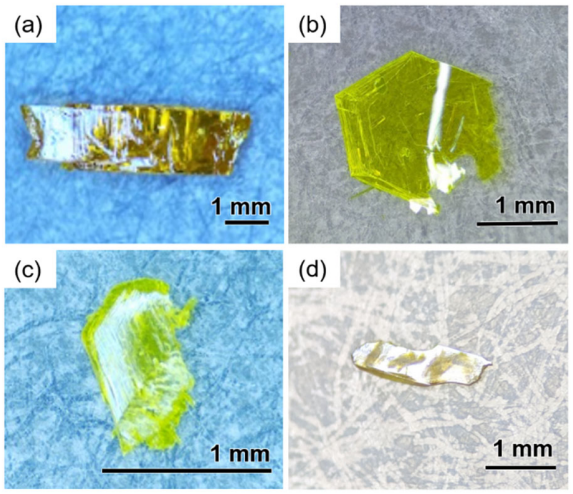

Figure 1. Appearance of the crystals. (a) DPAF-O grown by the naphthalene flux method, (b) DPAF-O grown by the PVT method, (c) DPAF-M grown by the PVT method, and (d) DTAF grown by the naphthalene flux method.

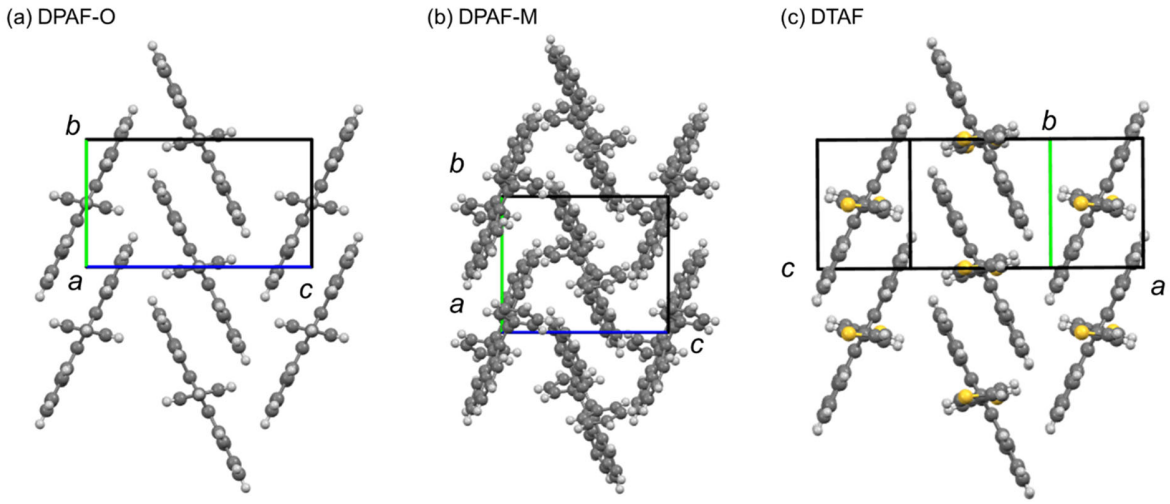

Figure 2. Crystal structure of (a) DPAF-O, (b) DPAF-M, and (c) DTAF.

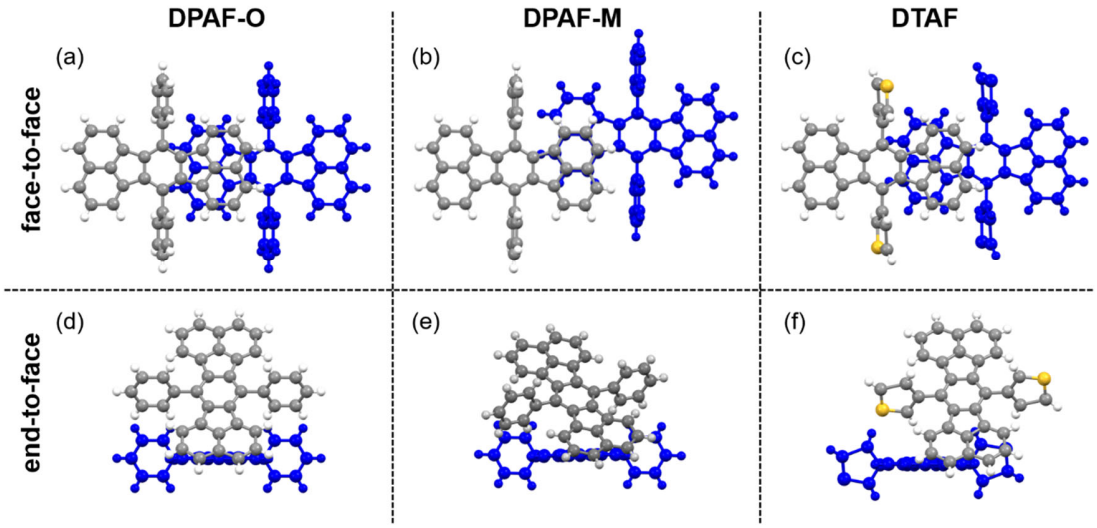

Figure 3. Molecular overlaps in face-to-face and end-to-face. (a), (d) DPAF-O, (b), (e) DPAF-M, (c), (f) DTAF.

Although the DPAF-M also forms a pitched π-stacking structure (Figure 2b), the crystallographic mirror symmetry in the pitched π-stacking layer is lost. Related to this, the overlap of molecules in the end-to-face direction differs from that of the DPAF-O (Figure 3e). The dihedral angle between molecules in the end-to-face direction is 44°. The stacking pattern in the π-stacking direction also differs significantly from that of the DPAF-O, with only a very small part of DPAF barely stacking face-to-face (Figure 3b). The interplanar distance between these molecules is 3.455 Å.

DTAF crystals were prepared by the naphthalene flux method (Figure S3). Like DPAF-O and DPAF-M crystals, DTAF also forms a pitched-π-stacking structure (Figure 2c). The space group is $P2_1/c$, and thienyl groups are disordered in the crystal. The overlapping structure of molecules in the π-stacking direction is almost the same as that of the DPAF-O, with an interplanar distance of 3.404 Å (Figure 3c). Unlike in the DPAF-O, the crystallographic mirror symmetry within the pitched π-stacking layer is lost (Figure 3f), and the molecules in the end-to-face direction are displaced in the molecular short axis. The dihedral angle between molecules in the end-to-face direction is 53°.

Calculation of intermolecular interaction

The crystal structures of AF-based molecules differ depending on the type of substituent. As previously reported, unsubstituted AF[45] and alkyl-substituted AF[30] molecules form a 1D stack structure, whereas DPAF and DTAF were here found to form a pitched π-stacking structure. The major difference between these two types of structures is the face-to-face molecular overlapping mode. Compared to the 1D stacking structure, in the pitched π-stacking structure, the molecules

are stacked face-to-face with a large displacement in the molecular long axis. In order to investigate the correlation between substituents and the face-to-face molecular overlapping mode, we calculated the intermolecular interactions (E_{int}) of the face-to-face molecular pairs at various positions of each molecule as follows.[46–50]

As shown in Figure 4, the origin, x-axis, y-axis, and z-axis were defined as the centroid of the molecule A, the molecular short axis, the molecular long axis, and the direction perpendicular to the molecular plane, respectively. As can be seen, molecule B was placed at z = 3.484 Å, the experimentally obtained interplanar distance, and the intermolecular interaction between molecule A and B was calculated by changing the position of molecule B in the xy-plane. In this calculation, molecule B was treated as a translation of molecule A, and the rotation of these molecules was not considered. The resulting 2D mapping of E_{int} shows the energetically favorable positions of the face-to-face pairs (Figure 5a). The minimum energy was obtained when molecule B was positioned at x=1.25, y=1.0Å. Such a molecular overlap with little displacement in the direction of the molecular long axis tended to give 1D stack structures. In fact, the reported 1D stacking structure of AF has a displacement of x=1.35, y=0.6 Å,[45] which is almost consistent with the value calculated here. No local minima were observed when the range of 2D mapping was expanded (Figure S6). Therefore, the π-stacking structure in the face-to-face direction of the crystal is found to be the most stable structure in terms of intermolecular interactions.

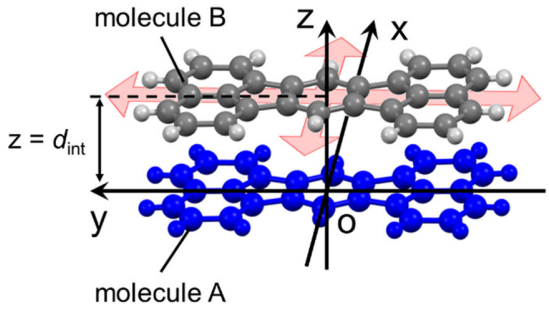

Figure 4. Schematic diagram of the dimer model for the calculation of face-to-face intermolecular interactions. The origin, x-axis, y-axis, and z-axis were defined as the centroid of the molecule, the molecular short axis, the molecular long axis, and the direction perpendicular to the molecular plane, respectively. The z coordinate of molecule B was fixed to the interplanar distance estimated from the experimentally obtained crystal structure. The intermolecular interaction between molecule A and B was calculated by changing the position of molecule B in the xy-plane.

Previous studies have shown that the crystal structure of the butyl-substituted AF is a 1D stacking structure (x=2.9, y=1.34Å).[30] In the present report, the stable dimer structure of butyl-substituted AF was found to have the lowest energy at x=2.5 and y=1.25 Å (Figure 5b). This is not significantly different from the energy of the unsubstituted molecule. Nevertheless, the energy was estimated to be approximately 10 kcal mol^{-1} lower than that of the unsubstituted AF, suggesting that intermolecular interactions between alkyl chains contribute to the stabilization in this case. In the 2D-E_{int} mapping of the unsubstituted AF, x=2.5 and y=1.25 are unstable, supporting the stabilization by alkyl chains in butyl-substituted AF. Thus, the attractive interactions between the alkyl chains suppress the displacement along the molecular long axis necessary for the formation of the pitched π-stacking structure (Figure S6).

In the case of DPAF (z=3.478 Å), the calculations showed that x=0, y=6.65 Å is the stable position (Figure 5c). This is in close agreement with the experimental value of DPAF-O (x=0, y=6.97Å). Therefore, it was suggested that the intermolecular interaction in the π-stacking direction is dominant in determining the crystal structure, even in the DPAF-O. The introduction of a phenyl group at the central position stabilizes the π-stacking structure with a large displacement along the molecular long axis, which is crucial in forming the pitched π-stacking structure. Such a slipped π-stacking structure is also observed in brickwork structure. A pseudo brickwork structure was prepared starting from the stable structure of the dimer model (details are shown in the SI), and its stability was compared with that of the experimentally obtained pitched π stacking structure; the pitched π stacking structure was much more stable than the brickwork structure (Figure S7). The experimentally obtained molecular overlap of the DPAF-M (x=2.24, y=8.13 Å) is not consistent with the intermolecular interaction minima (Figure S6), suggesting that the DPAF-M is stabilized by contributions other than intermolecular interactions in the π-stacking direction.

In the case of DTAF (z=3.404 Å), x=0, y=6.75 Å is the stable position (Figure 5d), which is in good agreement with the crystal structure (x=0.37, y=6.82 Å). The thienyl and phenyl groups were found to have the effect of forming π stacks that are displaced in the molecular long axis direction. The main reason for the difference in stable configuration depending on the substituent is probably the attractive interaction between the alkyl chains. In addition, in the case of alkyl groups, the two alkyl chains extend upward and downward, respectively, relative to the molecular plane, leaving space for displacement in the molecular short-axis direction. On the other hand, phenyl and thienyl groups provide steric hindrance that is approximately symmetrical vertically with respect to the

molecular plane, effectively suppressing displacement in the short-axis direction and inducing displacement in the long-axis direction.

The displacement in the molecular long axis direction of DPAF and DTAF is larger than that of rubrene. In the case of rubrene, the molecules are displaced by steric repulsion between phenyl groups, but in the case of DPAF and DTAF, the displacement is larger to avoid contact between the naphthalene moiety of the AF skeleton and the phenyl and thienyl groups. Such a displaced π-stacking structure is advantageous in the hopping mechanism because the distance between the molecular centroid becomes longer. In addition, since the molecules in the end-to-face direction are related by symmetry operation, the larger the displacement of the π-stacking molecules, the more acute the dihedral angles with the molecules in the end-to-face direction become. Therefore, the dihedral angles of DPAF and DTAF are more acute than those of rubrene.

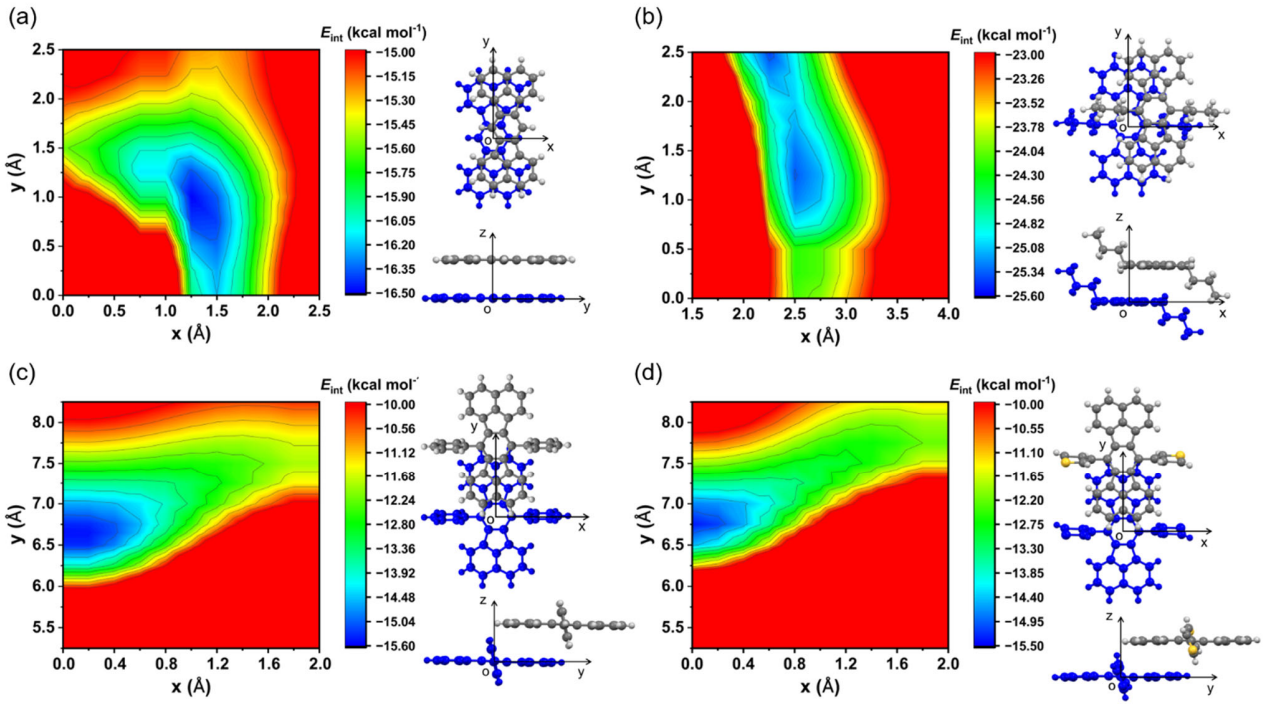

Figure 5. 2D mapping of the intermolecular interaction energy (E_{int}) of face-to-face pairs of (a) AF, (b) butyl-substituted AF, (c) DPAF, and (d) DTAF molecules. The definition of the coordinates is shown in Figure 4. The projections show the calculated most stable structure from the direction perpendicular to the molecular plane and from the direction parallel to the molecular plane.

Theoretical calculation of anisotropic mobility

The anisotropic carrier mobility based on the hopping model[41,42] can be calculated from the reorganization energy (λ) and intermolecular electronic coupling (V). The HOMO levels of DPAF and DTAF were estimated to be 5.40 and 5.49 eV, respectively, in the DFT calculations, suggesting that they are p-type materials. The λ values for hole transport of DPAF and DTAF were estimated to be 159 meV and 198 meV, respectively. Figure 6 shows electronic coupling (V) and anisotropic hole mobilities for the DPAF-O, DPAF-M and DTAF crystals. Interestingly, even though these crystals are all classified as having pitched π-stacking structure, the magnitude and dimensionality of the V are different for each crystal. The V values of the DPAF-M are small in all the directions, with the calculated mobility being as small as 0.17 $cm^2\ V^{-1}\ s^{-1}$ at maximum. The mobility anisotropy (μ_{min}/μ_{max}) is 1.8×10^{-2}. In DTAF, the V for the π-stacking direction is larger than in the DPAF-M, and the calculated mobility is relatively high with a maximum of 1.05 $cm^2\ V^{-1}\ s^{-1}$. However, the anisotropy remains high ($\mu_{min} / \mu_{max} = 2.0 \times 10^{-2}$). In contrast, in the DPAF-O the calculated V values are large in both the stack and end-to-face directions (about 30 meV). The maximum mobility is 0.50 and its anisotropy is very low (($\mu_{min} / \mu_{max} = 0.83$). This result suggests that the DPAF-O has a 2D electronic structure despite its pitched π-stacking structure.

These results can be explained by the difference in molecular packing and HOMO distribution (Figure S9). Comparing the molecular overlaps in the π-stacking direction, about a half of the AF skeleton of each molecule overlaps face-to-face in the case of the DPAF-O and DTAF, whereas only the ends of the molecules overlap in the case of the DPAF-M. As a result, the V in the π-stacking direction is reduced in the DPAF-M, although the HOMO is distributed in this slightly overlapping region. The V in the end-to-face direction reflects the overlap of orbitals between naphthalene moieties in the AF skeleton of each molecule. In the case of DPAF-M and DTAF, only a part of the naphthalene moieties overlaps due to their low symmetry (Figure 3e,f). On the other hand, in the case of DPAF-O, the naphthalene moieties overlap effectively because each molecule is located on a common mirror plane (Figure 3d). In addition, as shown in Figure S9, the HOMO phases are well matched in this overlap. As a result, only the DPAF-O has a large V in this direction as well.

The V in the end-to-face direction of DPAF-O is about twice that of rubrene, even though these crystals are isomorphic. This difference can be attributed to the molecular structure and the dihedral angle in the end-to-face direction. In the case of rubrene, the π skeleton, i.e., tetracene moiety, has only one benzene ring at the end, whereas the AF skeleton of DPAF has two benzene rings at the end, resulting in a wider distribution of molecular orbitals contributing to V in the end-to-face direction. The acute dihedral angle of DPAF-O compared to rubrene is also a major factor contributing to the large V.

On the other hand, unfortunately, the V in the π stacking direction in the DPAF-O is lower than that of rubrene. The reason for this is the mismatching of molecular orbitals in DPAF-O crystals. In the rubrene crystal, the HOMO phases are very well matched between the face-to-face overlapping molecules, which causes the high V of rubrene (Figure S10). In contrast, in the case

of DPAF-O, the belly of HOMO is stacked on top of the node, resulting in a smaller V in the π-stacking direction.[51,52] Thus, despite its pitched π-stacking structure, DPAF-O has a two-dimensional electronic state with extremely low anisotropy of mobility in the π-stacking and end-to-face directions.

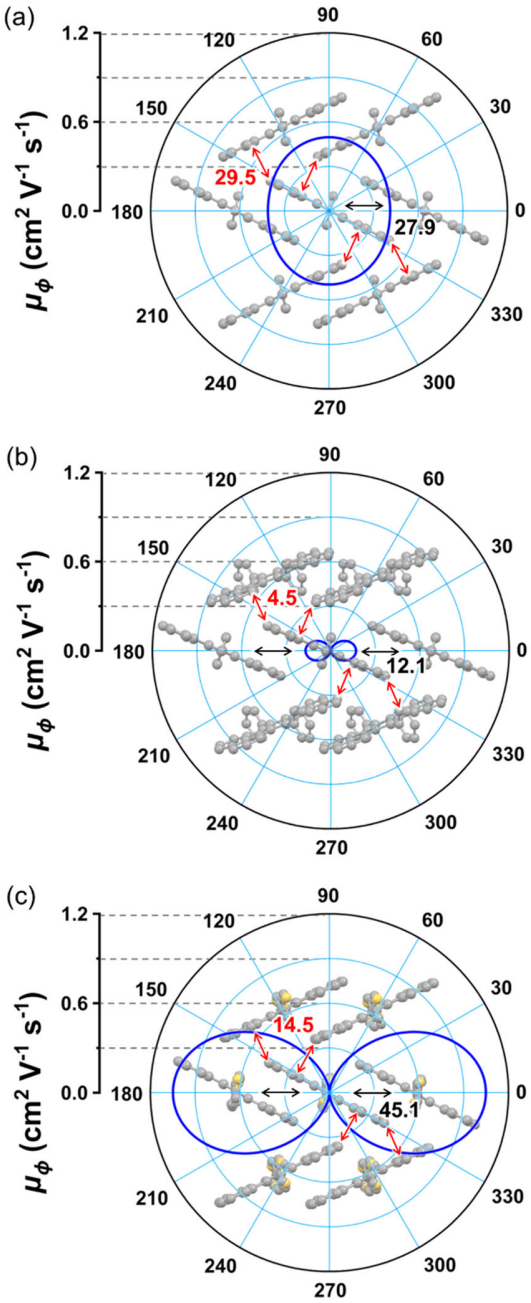

Figure 6. Calculated electronic coupling (*V*) and anisotropic hole mobilities of (a) DPAF-O, (b) DPAF-M, and (c)DTAF.

Single-crystal FETs of DPAF-O

Mobility anisotropy of the DPAF-O was investigated using SC-FETs. Film-like crystals of the DPAF-O obtained by PVT were used. Single crystal transistors of DPAF-M and DTAF could not be measured because of their thick crystals. The growth direction of the DPAF-O crystals corresponds to the π-stack axis. FET characteristics were measured parallel and perpendicular to the crystal growth direction as shown in the Figure 7. The dimensions of these two devices are shown in Figure S11. In both cases, DPAF SC-FETs exhibit p-type characteristics. Hole mobility is 0.52 in the parallel direction and 0.17 $cm^2 V^{-1} s^{-1}$ in the perpendicular direction, which is roughly in good agreement with the theoretical calculations. Thus, the theoretical calculations and experimental mobility measurements suggested that DPAF exhibits two-dimensional hole transport properties despite its pitched π-stacking structure. The transistor characteristics measured along the parallel direction have a larger hysteresis than those measured along the perpendicular direction. This suggests that the trap density in the crystal is inhomogeneous, but the origin of such a situation is not clear. Organic semiconductors with two-dimensional electronic states potentially exhibit band-like charge transport. However, in this system, the temperature dependence of the mobilities is thermally activated behavior (Figure S12), which suggested that the charge transport in DPAF-O is based on the hopping mechanism.

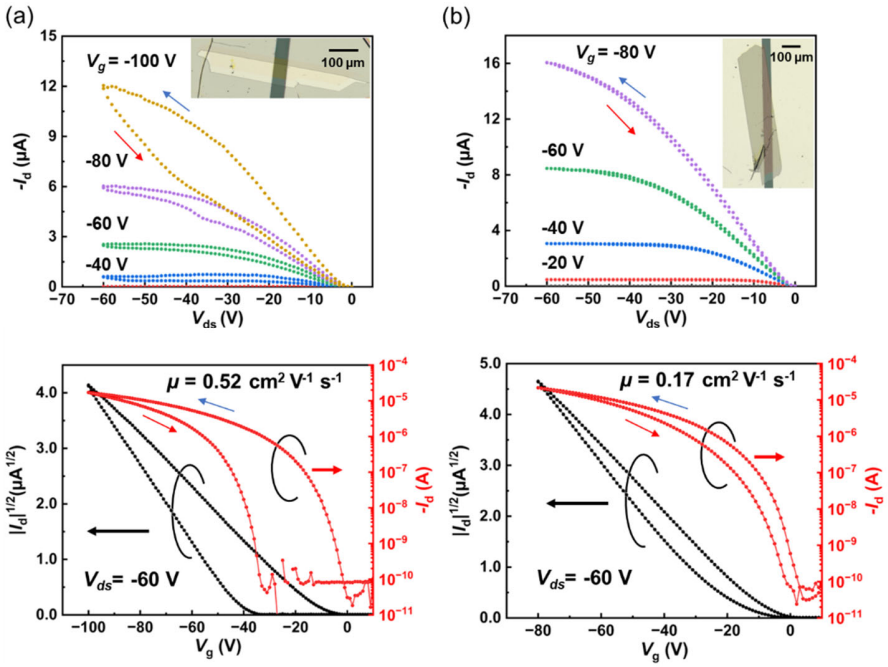

Figure 7. SC-FET characteristics of DPAF-O measured along directions (a) parallel and (b) perpendicular to the crystal growth direction. The insets are the photos of the devices. The gate capacitance per unit area was determined to be 6.01 nF cm^{-2}.

Conclusion

In addition to DPAF, DTAF was newly synthesized and three types of pitched π-stacking structures were obtained: the previously reported DPAF-O, the new polymorphic DPAF-M, and DTAF. To investigate the factors that cause these molecules to form pitched π-stacking structures, the intermolecular interactions of the face-to-face molecular pairs were calculated for each molecule. With the exception of DPAF-M, the calculated most stable face-to-face molecular pairs are in close agreement with the experimental orientations, suggesting that the intermolecular interactions of such dimers play a dominant role in determining the crystal structure. In butyl-

substituted AFs, the alkyl chains interact with each other to form π-stacks with little misalignment. On the other hand, DPAF and DTAF with phenyl or thienyl groups effectively induce π-stacks with large misalignment in the long-axis direction due to steric hindrance symmetrically distributed above and below the molecular plane. Such a slipped π-stacking structure is essential for the pitched π-stacking structure.

Theoretical calculations based on the hopping model for mobility anisotropy suggested that DPAF-M and DTAF form one-dimensional electronic states, whereas DPAF-O forms two-dimensional electronic states. We had assumed that the naphthalene moiety at the end of the AF skeleton would increase the electronic coupling in the end-to-face direction in the pitched π-stacking structure, but such an effect is limited to highly symmetric crystals such as DPAF-O. The electron coupling in the end-to-face direction of DPAF-O is about twice that of rubrene in isomorphous crystals, suggesting that the introduction of a naphthalene moiety contributes to increased electron coupling in this direction. Actually, isotropic mobility was observed in SC-FETs with DPAF-O. This research shows that molecular design that introduces a wide π-conjugated moiety at the end of the molecule is effective in making the electronic state of the pitched π-stacking structure two-dimensional. In order to make such wide π-conjugation at the molecular ends effective for electronic coupling, it will be important to design molecules more precisely to obtain crystal structures with high symmetry.

ASSOCIATED CONTENT

Supporting Information.

The following files are available free of charge.

Additional information for material synthesis, crystallization by the naphthalene flux method, crystallographic data, theoretical calculation of intermolecular interaction, molecular orbital overlaps and OFETs data (PDF)

Crystallographic data for DPAF-O (CIF)

Crystallographic data for DPAF-M (CIF)

Crystallographic data for DTAF (CIF)

AUTHOR INFORMATION

Corresponding Author

Seiya Yokokura: Graduate School of Chemical Sciences and Engineering, Hokkaido University, Kita 13 Nishi 8, Kita-ku, Sapporo, 060-8628, Japan; Division of Applied Chemistry, Faculty of Engineering, Hokkaido University, Kita 13 Nishi 8, Kita-ku, Sapporo, 060-8628, Japan

Email: seiyayokokura@eng.hokudai.ac.jp

Toshihiro Shimada: Graduate School of Chemical Sciences and Engineering, Hokkaido University, Kita 13 Nishi 8, Kita-ku, Sapporo, 060-8628, Japan; Division of Applied Chemistry, Faculty of Engineering, Hokkaido University, Kita 13 Nishi 8, Kita-ku, Sapporo, 060-8628, Japan

Email: shimadat@eng.hokudai.ac.jp

Present Addresses

Taro Nagahama:

†Graduate School of Sciences and Technology for Innovation, Yamaguchi University, Ube, Yamaguchi, 755-8611, Japan

Author Contributions

T.Y. performed the synthesis, crystallization, transistor measurements and theoretical calculation. M.J. contributed to the XRD measurement. S.Y. and T.S. designed the present research, and S.Y., H. W., T.N. and T. S. prepared the manuscript.

Notes

The authors declare no competing financial interest.

ACKNOWLEDGMENT

This work was supported by a JSPS KAKENHI Grant (no. 23K13714) and a grant from the Iketani Science and Technology Foundation. The computation was performed using Research Center for Computational Science, Okazaki, Japan (Project: 22-IMS-C088, 23-IMS-C076) and the Supercomputer Center, the Institute for Solid State Physics, The University of Tokyo (2022-Ba--0061,2023-Ba-0051,2023-Bb-0020).

REFERENCES

1 Mazaki, Y.; Kobayashi, K. Crystal and Molecular Structure of Thieno[Z",3" : 4‘,5‘]thieno[2’,3’-d]thieno- [3,2-b]thiophene as a Hydrogen-poor Heterocycle. *J. Chem. Soc., Perkin Trans*. 2, 1992, 1., 761-764.

2 Takimiya, K.; Bulgarevich, K.; Abbas, M.; Horiuchi, S.; Ogaki, T.; Kawabata, K.; Ablat, A. “Manipulation” of Crystal Structure by Methylthiolation Enabling Ultrahigh Mobility in a Pyrene-Based Molecular Semiconductor. *Adv. Mater*. 2021, 33, 2102914.

3 Mattheus, C. C.; De Wijs, G. A.; de Groot, R. A.; Palstra T. T. M. Modeling the Polymorphism of Pentacene. *J. Am. Chem. Soc.* 2003, 125, 6323-6330.

4 Kumar, S.; Huang, D.; Venkateswarlu, S.; Tao Y. Nonlinear Polyfused Aromatics with Extended π-Conjugation from Phenanthrotriphenylene, Tetracene, and Pentacene: Syntheses, Crystal Packings, and Properties. *J. Org. Chem*. 2018, 83, 11614−11622.

5 Park, S. K.; Kim, J. H.; Park, S. Y. Organic 2D Optoelectronic Crystals: Charge Transport, Emerging Functions, and Their Design Perspective. *Adv. Mater*. 2018, 30, 1704759.

6 Mamada, M.; Katagiri, H.; Sakanoue, T.; Tokito, S. Characterization of New Rubrene Analogues with Heteroaryl Substituents. *Cryst. Growth Des*. 2015, 15, 442−448.

7 Chi, X.; Li, D.; Zhang H.; Chen Y.; Garcia, V.; Garcia, C.; Siegrist, T. 5,6,11,12-Tetrachlorotetracene, a tetracene derivative with p-stacking structure: The synthesis, crystal structure and transistor properties. *Org. Electron.* 2008, 9, 234–240.

8 Ogden, W. A.; Ghosh, S.; Bruzek, M. J.; McGarry, K. A.; Balhorn, L.; Young, V. Jr.; Purvis, L. J.; Wegwerth, S. E.; Zhang, Z.; Serratore, N. A.; Cramer, C. J.; Gagliardi, L.; Douglas, C. J. Partial Fluorination as a Strategy for Crystal Engineering of Rubrene Derivatives. *Cryst. Growth Des*. 2017, 17, 643−658.

9 Holmes, D.; Kumaraswamy, S.; Matzger, A. J.; Vollhardt, K. P. C. On the Nature of Nonplanarity in the [N]Phenylenes. *Chem. Eur. J*. 1999, 5, 3399-3412.

10 Pithan, L.; Nabok, D.; Cocchi, C.; Beyer, P.; Duva, G.; Simbrunner, J.; Rawle, J.; Nicklin, C.; Schäfer, P.; Draxl, C.; Schreiber, F.; Kowarik, S. Molecular structure of the substrate-induced thin-film phase of tetracene. *J. Chem. Phys.* 2018, 149, 114701.

11 Butko, V. Y.; Chi, X.; Ramirez, A. P. Free-standing tetracene single crystal field effect transistor. *Sol. St. Comm.* 2003, 128, 431–434.

12 de Boer, R. W. I.; Klapwijk, T. M.; Morpurgo, A. F. Field-effect transistors on tetracene single crystals. *Appl. Phys. Lett*. 2003, 83, 4345–4347

13 Goldmann, C.; Haas, S.; Krellner, C.; Pernstich, K. P.; Gundlach, D. J.; Batlogg, B. Hole mobility in organic single crystals measured by a "flipcrystal" field-effect technique. *J. Appl. Phys*. 2004, 96, 2080–2086.

14 Xia, Y.; Kalihari, V.; Frisbie, C. D.; Oh, N. K.; Rogers, J. A. Tetracene air-gap single-crystal field-effect transistors *Appl. Phys. Lett.* 2007, 90, 162106

15 Reese, C.; Chung, W. J.; Ling, M. M.; Roberts, M.; Bao, Z. High-performance microscale single-crystal transistors by lithography on an elastomer dielectric. *Appl. Phys. Lett.* 2006, 89, 202108

16 Uttiya, S.; Miozzo, L.; Fumagalli, E. M.; Bergantin, S.; Ruffo, R.; Parravicini, M.; Papagni, A.; Moret, M.; Sassella, A. Connecting molecule oxidation to single crystal structural and charge transport properties in rubrene derivatives. J. *Mater. Chem. C*, 2014, 2, 4147–4155.

17 Bergantin, S.; Moret, M. Rubrene Polymorphs and Derivatives: The Effect of Chemical Modification on the Crystal Structure. *Cryst. Growth Des*. 2012, 12, 6035−6041.

18 Wang, X.; Garcia, T.; Monaco, S.; Schatschneider, B.; Marom, N. Effect of crystal packing on the excitonic properties of rubrene polymorphs. *Cryst. Eng. Comm*. 2016, 18, 7353–7362.

19 Takeya, J.; Yamagishi, M.; Tominari, Y.; Hirahara, R.; Nakazawa, Y.; Nishikawa, T.; Kawase, T.; Shimoda, T.; Ogawa S. Very high-mobility organic single-crystal transistors with incrystal conduction channels. *Appl. Phys. Lett*. 2007, 90, 102120.

20 Podzorov, V.; Menard, E.; Borissov, A.; Kiryukhin, V.; Rogers, J. A.; Gershenson, M. E. Intrinsic Charge Transport on the Surface of Organic Semiconductors. Phys. Rev. Lett. 2004, 93, 086602.

21 Sundar, V. C.; Zaumseil, Z.; Podzorov, V.; Menard, E.; Willett, R. L.; Someya, T.; Gershenson, M. E.; Rogers, J. A. Elastomeric Transistor Stamps: Reversible Probing of Charge Transport in Organic Crystals. *Science.* 2004, 303, 5664.

22 Zhang, Y.; Dong, H.; Tang, Q.; Hea, Y.; Hu, W. Mobility dependence on the conducting channel dimension of organic field-effect transistors based on single-crystalline nanoribbons. *J. Mater. Chem.*, 2010, 20, 7029–7033.

23 Takenaka, H.; Ogaki, T.; Wang, C.; Kawabata, K.; Takimiya K. Selenium-Substituted β-Methylthiobenzo[1,2-b:4,5-b′]dithiophenes: Synthesis, Packing Structure, and Transport Properties. *Chem. Mater.* 2019, 31, 6696−6705.

24 Wang, C.; Nakamura, H.; Sugino, H.; Takimiya K. Methylthionated benzo[1,2-b:4,5-b0]dithiophenes: a model study to control packing structures and molecular orientation in thienoacene-based organic semiconductors. *Chem. Commun.,* 2017, 53, 9594—9597.

25 Wang, C.; Hashizume, D.; Nakano, M.; Ogaki, T.; Takenaka, H.; Kawabata, K.; Takimiya, K. "Disrupt and induce" intermolecular interactions to rationally design organic semiconductor crystals: from herringbone to rubrene-like pitched pstacking. *Chem. Sci*., 2020, 11, 1573–1580.

26 Kanazawa, K.; Bulgarevich, K.; Kawabata, K.; Takimiya, K. Uncovered Effects of thieno[2,3-b]thiophene Substructure in a Tetrathienoacene Backbone: Reorganization Energy and Intermolecular Interaction. *Chem. Mater*. 2023, 35, 280−288.

27 Kanazawa, K.; Bulgarevich, K.; Kawabata, K.; Takimiya, K. Methylthiolation of Acenes: Change of Crystal Structure from Herringbone to Rubrene-like Pitched π-Stacking Structure. *Cryst. Growth Des*. 2023, 23, 5941−5949.

28 Seth, S.; Sur, H.; Chakraborty, S. The Structure of 7,14-Di-n-propylacenaphtho[1,2-k]fluoranthene. *Acta Cryst. C.* 1988, 44, 1011-1014.

29 Seth, S.; Chakraborty, S. Structure of 7,1 4-Dibutylaeenaphtho[1,2-k]fluoranthene. *Acta Cryst.* B. 1981. 37, 1144-1146.

30 Seth, S.; Chakraborty, S. The Structure of 7,14-Di-n-pentylacenaphtho[1,2-k]fluoranthene, $C_{36}H_{34}$. *Acta Cryst.* C. 1983. 39, 625-627.

31 Kunugi, Y.; Kosuge, T.; Okamoto, K. Characterization of Vapor-Deposited Acenaphtho[1,2-k]fluoranthene Derivative Films as Active Layers of Organic Field-Effect Transistors. Electrochemistry. 2008, 12, 865-867

32 Watson, W. H.; Kashyap, R. P. Structures of 7,10-Diphenylfluoranthene and 7,14-Diphenylacenaphtho[1,2-k]fluoranthene. *Acta Cryst. C.* 1991, 47, 1848-1851.

33 Wehmeier, M.; Wagner, M.; Müllen, K. Novel Perylene Chromophores Obtained by a Facile Oxidative Cyclodehydrogenation Route. *Chem. Eur. J*. 2001, 7, 10, 2197-2205.

34 Yanase, T.; Tanoguchi, H.; Sakai, N.; Jin, M.; Yamane, I.; Kato, Masaki.; Ito, H.; Nagahama, T.; Shimada, T. Single Crystal Growth of π-Conjugated Large Molecules without Solubilizing Alkyl Chains via the Naphthalene Flux Method. *Cryst. Growth Des*. 2021, 21, 4683−4689.

35 Yang, X.; Li, M.; Maeno, A.; Yanase, T.; Yokokura, S.; Nagahama, T.; Shimada, T. Growth of Pentacene Crystals by Naphthalene Flux Method. *ACS Omega.* 2022, 7, 28618-28623.

36 Tanoguchi, H.; Yuki, T.; Yokokura, S.; Yanase, T.; Jin, M.; Ito, H.; Nagahama, T.; Shimada, T. Single Crystal Growth of Cyclopenta-Fused Polycyclic Aromatic Hydrocarbon by the Naphthalene Flux Method: 2D Ambipolar Charge Transport Properties and NIR Absorption. *ACS Appl. Electron. Mater*. 2023, 5, 6266−6274.

37 Dolomanov, O. V.; Bourhis, L. J.; Gildea, R. J.; Howard, J. A. K.; Puschmann, H. OLEX2: a complete structure solution, refinement and analysis program. *J. Appl. Cryst*. 2009, 42, 339–341

38 Sheldrick., G. M. Crystal structure refinement with SHELXL. *Acta Cryst. C.* 2015, 71, 3–8.

39 Grimme, S.; Antony, J.; Ehrlich, S.; Krieg, H. A consistent and accurate ab initio parametrization of density functional dispersion correction „DFT-D… for the 94 elements H-Pu. *J. Chem. Phys*. 2010, 132, 154104.

40 Peverati, R.; Baldridge, K. K. Implementation and Performance of DFT-D with Respect to Basis Set and Functional for Study of Dispersion Interactions in Nanoscale Aromatic Hydrocarbons. *J. Chem. Theory Comput.* 2008, 4, 2030-2048.

41 Wen, S.; Li, A.; Song, J.; Deng, W.; Han, K.; Goddard III, W. A. First-Principles Investigation of Anistropic Hole Mobilities in Organic Semiconductors. J. Phys. Chem. B, 2009, 113, 8813-8819.

42 Nguyen, T. P.; Shim, J. H.; Lee, J. Y. Density Functional Theory Studies of Hole Mobility in Picene and Pentacene Crystals. *J. Phys. Chem. C* . 2015, 119, 11301−11310.

43 Mei, Y.; Fogel, D.; Chen, J.; Ward, J. W.; Payne, M. M.; Anthony, J. E.; Jurchescu, O. D. Interface engineering to enhance charge injection and transport in solution-deposited organic transistors. Org. Electron. 2017, 50, 100-105

44 Jurchescu, O. D.; Meetsma A.; Palstra, T. T. M. Low-temperature structure of rubrene single crystals grown by vapor transport. *Acta Cryst. B.* 2006, 62, 330–334.

45 Akhmetov, V.; Feofanov, M.; Papaianina, O.; Troyanov, S.; Amsharov, K. Towards Nonalternant Nanographenes through Self-Promoted Intramolecular Indenoannulation Cascade by C−F Bond Activation. *Chem. Eur. J*. 2019, 25, 11609 – 11613.

46 Hutchison, G. R.; Ratner, M. A.; Marks, T. J. Intermolecular Charge Transfer between Heterocyclic Oligomers. Effects of Heteroatom and Molecular Packing on Hopping Transport in Organic Semiconductors. *J. Am. Chem. Soc*. 2005, 127, 16866-16881.

47 Gryn'ova, G.; Corminboeuf, C. Implications of Charge Penetration for Heteroatom-Containing Organic Semiconductors. *J. Phys. Chem. Lett.* 2016, 7, 5198−5204.

48 Thorley, K. J.; Risko, C. On the impact of isomer structure and packing disorder in thienoacene organic semiconductors. *J. Mater. Chem. C*, 2016, 4, 4040-4048.

49 Takimiya, K.; Kanazawa, K.; Kawabata, K. Crystal Structures of β-Methylchalcogenated Tetrathienoacenes: From One-Dimensional π-Stacking to Sandwich Pitched π-Stacking Structure. *Cryst. Growth Des*. 2021, 21, 4055−4063.

50 Bulgarevich, K.; Horiuchi, S.; Takimiya, K. Crystal-Structure Simulation of Methylthiolated Peri-Condensed Polycyclic Aromatic Hydrocarbons for Identifying Promising Molecular Semiconductors: Discovery of 1,3,8,10-tetrakis(methylthio)peropyrene Showing Ultrahigh Mobility. *Adv. Mater*. 2023, 2305548.

51 Dong, H.; Fu, X.; Liu, J.; Wang, Z.; Hu, W. 25th Anniversary Article: Key Points for High-Mobility Organic Field-Effect Transistors. *Adv. Mater*. 2013, 25, 6158–6183.

52 Coropceanu, V.; Cornil, J.; da Silva Filho, D. A.; Olivier, Y.; Silbey, R., Brédas, J. Charge Transport in Organic Semiconductors. *Chem. Rev.* 2007, 107, 926−952.

For Table of Contents Use Only

Pitched π-stacking crystal structure and two-dimensional electronic structure of acenaphtho[1,2-k]fluoranthene analogues with various substituents

Takuma Yuki,[1] Seiya Yokokura,[1,2,*] Mingoo Jin,[3] Hiroki Waizumi,[1,2] Taro Nagahama, [1,2,] Toshihiro Shimada[1,2,*]

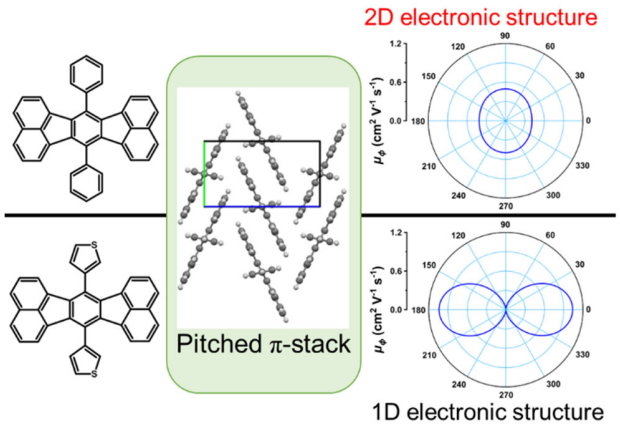

SYNOPSIS

7,14-diphenylacenaphtho[1,2-k]fluoranthene (DPAF) and its analogues were synthesized and crystallized. The correlation between substituents and crystal structures and electronic states of the previously reported and synthesized molecules were explored experimentally and theoretically. DPAF crystal was found to form a two-dimensional electronic structure in spite of its pitched π-stacking structure.